Polyaniline-Based Flexible Sensor for pH Monitoring in Oxidizing Environments

Liam Bignall, Claire Magnenet, Catheline Ramsamy, Sophie Lakard, Simon Vassal, Boris Lakard

chemosensors

Article

Polyaniline-Based Flexible Sensor for pH Monitoring in Oxidizing Environments

Liam Bignall [1], Claire Magnenet [2], Catheline Ramsamy [1], Sophie Lakard [2], Simon Vassal [1] and Boris Lakard [2,*]

[1] Linxens Holding, 78200 Mantes-La-Jolie, France; liam.bignall@linxens.com (L.B.); catheline.ramsamy@linxens.com (C.R.); simon.vassal@linxens.com (S.V.)
[2] Institut UTINAM, Université de Franche-Comté, Centre National de la Recherche Scientifique, 25000 Besançon, France; claire.magnenet@univ-fcomte.fr (C.M.); sophie.lakard@univ-fcomte.fr (S.L.)
* Correspondence: boris.lakard@univ-fcomte.fr

Abstract: Measuring pH in oxidizing solutions is a crucial issue in areas such as aquaculture, water treatment, industrial chemistry, and environmental analysis. For this purpose, a low-cost potentiometric flexible sensor using a polymer film as a pH-sensitive material has been developed in this study. The sensor consists in a polyaniline film electrodeposited from a sulfuric acid solution on a gold electrode previously deposited on a flexible polyimide substrate. The resulting polyaniline-based pH sensors showed an interesting performance detection in aqueous solution, leading to sensitive (73.4 mV per unit pH) and reproducible (standard deviation of 1.75) responses over the entire pH range from 3 to 8. On the contrary, they were inoperative in the presence of oxidizing hypochlorite ions. Thus, other polyaniline films were electrodeposited in the presence of cetyltrimethylammonium bromide or Tritonx100 surfactant in an attempt to improve the sensing performance of the pH sensors in oxidizing solutions. The pH sensors based on polyaniline and Tritonx100 surfactant were then found to be sensitive (62.3 mV per unit pH) and reproducible (standard deviation of 1.52) in aqueous solutions containing hypochlorite ions. All polyaniline films were also characterized by profilometry and electronic microscopy to correlate the physicochemical features with the performance of the sensors.

Keywords: flexible sensors; pH sensors; polyaniline; surfactants; electrochemistry

Citation: Bignall, L.; Magnenet, C.; Ramsamy, C.; Lakard, S.; Vassal, S.; Lakard, B. Polyaniline-Based Flexible Sensor for pH Monitoring in Oxidizing Environments. *Chemosensors* **2024**, *12*, 97. https://doi.org/10.3390/chemosensors12060097

Received: 19 April 2024
Revised: 30 May 2024
Accepted: 1 June 2024
Published: 3 June 2024

1. Introduction

The concept of pH was introduced by Sørensen in 1909. Sørensen defined pH as the negative logarithm of the concentration of hydrogen ions in a solution while studying the effect of hydrogen ion concentration on the enzyme activity of yeast [1]. Later, the definition of pH was modified, since the concentration was replaced by the activity to consider the interactions between ions within a solution, which makes the ions deviate from an ideal behavior, as modeled by Debye and Hückel in 1923 [2]. The first pH glass membrane electrode was developed by Haber and Klemensiewicz in 1909 [3] and incorporated into the first pH-meter developed and commercialized by Beckham [4]. The invention of the pH glass electrode revolutionized pH measurement, providing an accurate and reliable method compared to traditional chemical indicators and pH measurement gradually became essential to control and optimize reactions involved in biological processes, environmental monitoring, and industrial processes. Indeed, pH regulation is essential for enzymatic function and physiological balance [5,6], while pH monitoring makes it possible to control industrial processes to ensure the safety of products in the agri-food sector [7,8]. In addition, pH measurement makes it possible to better manage agricultural soils [9,10], but also to contribute to environmental monitoring through the assessment of water quality or ecosystem health [11,12].

Despite its reliability, the pH glass electrode suffers from several disadvantages, such as frequent calibrations, the fragility of the membrane glass that can degrade due to friction or

in harsh environments such as reactors, and its inability to operate in complex or confined environments, including biological systems. This is why alternative pH measurement systems continue to be developed. Thus, optical pH sensors use pH-sensitive species, usually a dye embedded in a polymer, that undergo reversible changes in their optical properties (refraction index, polarization, UV/Vis absorbance, fluorescence emission, etc.) in response to pH variations. When the sensor is exposed to a sample solution, the chemical species reacts with the hydrogen ions present in the solution, resulting in a change in the measurable optical properties that can be monitored using optical methods such as absorbance or fluorescence spectroscopy. The optical pH sensors generally provide rapid response times, are efficient over a wide range of pH values, are non-invasive, and require a low maintenance, but they are frequently expensive, have a limited accuracy especially when measuring in turbid or colored solutions, and their measurements can be disturbed by ionic strength interferences [13–15]. ISFET (Ion-Sensitive Field Effect Transistor) are another type of sensors that can be used for pH monitoring. Unlike traditional glass electrodes, ISFET sensors use a solid-state sensitive element, usually a metal oxide such as silicon dioxide, tantalum oxide, or titanium oxide. Indeed, such metal-oxide-based solid-state pH sensors rely on the adsorption of hydrogen ions onto the surface of the oxide layer, causing changes in the electrical properties of the sensitive material [16–18]. ISFET pH sensors offer significant benefits, including miniaturization, robustness, fast response times, reduce the acidic or alkaline errors in extreme pH, and can be stored dry. Nevertheless, they are expensive, do not offer the same accuracy than glass pH electrodes, have a drifting problem, are highly temperature dependent, and should not be used in solutions containing chlorine or other chemicals that damage the ISFET transistor. Other solid-state pH sensors use conductive polymers as a sensitive layer that may undergo reversible protonation and deprotonation reactions in response to changes in hydrogen ion activity in the solution. These reactions result in a variation of the potential measured by the sensor, which generally allows an accurate measurement of the pH. Thus, electrodeposited conductive polymers can be considered good candidates as a sensitive layer of pH sensors, as they are strongly bound to the surface of the sensors during the electropolymerization and due to the presence of amino groups, for example in polyaniline [19,20] and polydopamine [21], or carboxyl groups, for example in poly(11-N-pyrrolylundecanoic) acid [22], leading to protonation and deprotonation reactions. These sensors have several advantages, including fast response times, low detection limits, and resistance to fouling. However, they frequently suffer from the influence of certain interferents in specific media which may persist and require optimization [23–25].

Flexible sensors are becoming more and more important today due to their lightness, conformability, wearability, customizability, and versatility. In particular, flexible sensors can be integrated into clothing, accessories, and even directly onto the human body, allowing continuous monitoring of vital signs, movements, and environmental factors that pave the way for applications in the areas of sports performance monitoring [26,27], health [27–29], and personal safety through the identification of hazards in the environment [30,31]. In addition, conductive polymers and flexible sensors are inherently compatible, since both have mechanical flexibility, allowing them to bend, stretch, and deform along with the flexible substrate or structure of the sensor [32–34]. Also, conductive polymers, such as polyaniline, are lightweight, resistant, and can be deposited on flexible substrates either by chemical oxidation if the flexible substrate is insulating or by electrochemistry if the substrate is conductive [35,36].

Considering on the one hand the advantages of using polyaniline as a sensitive layer of pH sensors and on the other hand the interest in using flexible electrodes for applications in healthcare, sports, and safety, we therefore developed polyaniline-based flexible sensors in this work. The flexible electrodes were fabricated using a photolithographic process followed by a chemical etching which constitute an innovative alternative to standard screen-printed or sputtered electrodes. The process resulted in the obtention of flexible polyimide copper-based electrodes coated with a film of gold on which a polyaniline film

was electrochemically deposited. Then, the PANI-modified electrodes were successfully tested as pH sensors from pH 3 to 8 by using the open circuit potential technique (OCP). The potentiometric response to pH changes of PANI-modified electrodes were also tested in the presence of hypochlorite ions, a species that constitutes a major interferent in pH measurements in various fields, including aquaculture, water treatment, industrial chemistry, and environmental analysis. Since the response of polyaniline films electrosynthesized from sulfuric acid solutions was disturbed by the presence of hypochlorite ions, other polyaniline films were electrosynthesized in the presence of a surfactant, which allowed to strongly reduce the impact of the interferent on the potentiometric response of the pH sensors.

2. Materials and Methods

2.1. Materials and Reagents

Aniline monomer (>99.5%), Cetyltrimethylammonium bromide (>99%, CTAB), and Tritonx100 (>99.5%) were purchased from Acros Organics (Geel, Belgium). Sulfuric acid (98%) was purchased from ITW Reagents (Darmstadt, Germany) and Sodium hypochlorite was purchased from Sigma Aldrich (Saint-Quentin-Fallavier, France). Potassium phosphate monobasic (99%), potassium phosphate dibasic (99%), sodium carbonate decahydrate (>99.9%), hydrochloric acid (37%), and sodium hydroxide (0.1 M) were purchased from Thermo Fisher Scientific (Illkirch-Graffenstaden, France). Phosphate buffer solution (PBS) was homemade (PBS; 0.2 M KH_2PO_4 and 0.2 M K_2HPO_4, pH 6.0). The water used in all the experiments was deionized by a Synergy® water purification system (Milli-Q water of 18.2 MΩ cm resistivity, Merck, Darmstadt, Germany).

2.2. Flexible Chips

The flexible chips were fabricated by Linxens® (Mantes la Jolie, France). These chips are based on a process enabling the large-scale manufacturing of customer-specific flexible printed circuit boards, which has proven to be an excellent and cost-effective alternative to standard screen printed or sputtered electrodes. Linxens electrodes are composed of polyimide 50 µm and a sheet of copper of 15–18 µm glued onto the substrate (Figure 1a) and patterned to the desired design using a photolithographic process followed by a chemical etching (Figure 1b). The resulting conductive traces can then be used as a seed layer on top of which a 4-µm-thick layer of nickel is electroplated (Figure 1c). Then, a functional gold layer (200 nm) is applied selectively to ensure the right coverage of the under layers on the sensing area (Figure 1d), while a thinner layer is deposited on the non-functional areas leading to a cost optimized design. The resulting electrodes (Figure 1e,f) can then be used as (bio)sensors for the detection of various analytes while their low cost makes it possible to consider a single use of these sensors.

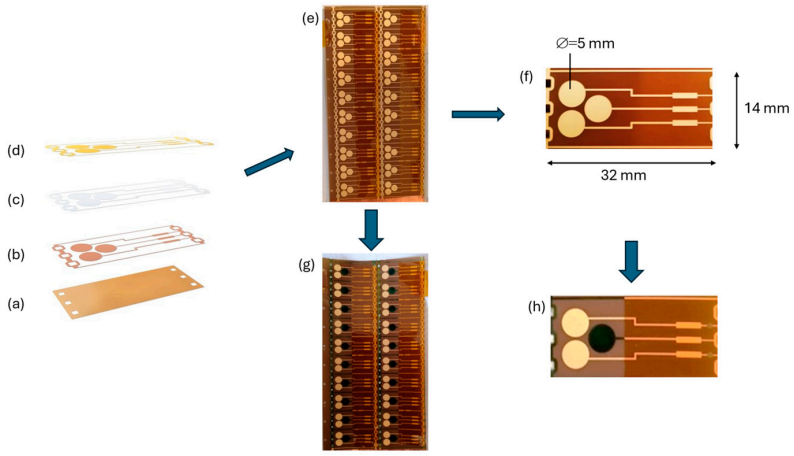

Figure 1. Fabrication process of flexible chips (**a**–**d**) and photographs of the flexible chips containing three independent electrodes before (**e**,**f**) and after (**g**,**h**) the electrodeposition of polyaniline films.

2.3. Electrochemical Polymerization

The electrodes were degreased by immersion for 20 s in a basic solution of sodium carbonate decahydrate concentrated at 0.5 M and heated to 50 °C, rinsed in water, immersed for 20 s in an acidic solution of sulfuric acid concentrated at 0.5 M, heated to 40 °C, and rinsed in water.

After that, the electrochemical polymerization of aniline (0.1 M) was carried out in an aqueous solution of sulfuric acid (1 M), sometimes with the addition of a surfactant (CTAB or Tritonx100) concentrated at 0.01 M. The electrochemical cell consists of a two-electrode setup with a platinum-plated titanium grid (16 × 4 × 0.1 cm) as the counter-electrode and a 20-chip board as the working electrode. The current was applied using either a dual power supply (ALR 3003 from ELC, Annecy, France) or a data acquisition and multimeter unit (DAQ6510 from Keithley, Les Ulis, France). After electrodeposition, the polyaniline films were deprotonated by immersion in a phosphate buffer solution (PBS 0.2 M, pH 6) to enhance their response to pH changes during detection tests.

2.4. Analytical Techniques

Mechanical Profilometry. The thickness of the gold electrodes and polyaniline-modified gold electrodes was measured by mechanical profilometry using a Bruker's Dektak® (Karlsruhe, Germany) stylus profiler with the Vision 64 software. Each thickness was measured on a scan length of 1000 µm at a scan speed of 25 µm·s^{-1} (stylus radius: 2 µm, stylus force: 3 mg).

Scanning Electron Microscopy (SEM). The surface morphology of gold electrodes and polyaniline-modified gold electrodes was obtained, without prior metallization, using a high-resolution scanning electron microscope Quanta 450 W from FEI with an electron beam energy of 5 keV and a working distance of 10 mm.

Potential Measurements. A portable Sensit Smart potentiostat, from PalmSens® (Houten, The Netherlands), was connected to a computer via a USB bus and controlled by the PSTrace software (https://www.palmsens.com/software/ps-trace/). The Linxens electrodes were connected to the potentiostat using PalmSens connectors with banana receptacles. Potentiometric measurements were made in pH solutions ranging from pH 3 to pH 8 using a Linxens working electrode and an Ag/AgCl reference electrode with 3 M KCl as reference electrolyte. For each pH value, the potential was recorded versus time for one minute at room temperature (22 ± 1 °C). The pH of the solution was adjusted by addition of HCl (0.1 M) or NaOH (0.1 M).

3. Results and Discussion

3.1. Preparation and Characterization of the Polyaniline Films Electrodeposited on the Gold Electrodes of the Chips

After degreasing in a basic bath and then in an acid bath, a board containing 20 chips was immersed in an electrolyte composed of sulfuric acid (1 M) and aniline (0.1 M). A potential of +1 V was then applied to the electrolyte for 60 s leading to the deposition of a thin pale green polyaniline film. The entire board was then thoroughly rinsed with water. After that, a potential of +1.3 V was applied to the electrolyte for 60 s leading to the electrodeposition of a thicker film of dark green polyaniline denoted PANI/H_2SO_4 (Figure 1g,h). The board was rinsed again thoroughly with water. Then, the chips were immersed in a PBS solution (pH 6.0) for 90 min. Similarly, polyaniline films were electrodeposited on the electrodes from solutions composed of aniline, H_2SO_4, and a surfactant, but they were electrodeposited by applying a potential of +1.3 V to the electrolyte for 120 s. The surfactant used was either CTAB, an anionic surfactant likely to act as a counter-anion doping polymer film, or Tritonx100, a neutral surfactant that improved monomer solubility. The resulting polymer films are denoted PANI/H_2SO_4 + CTAB and PANI/H_2SO_4 + Tritonx100. In addition, a previous study showed that the presence of surfactants in the electrolyte does not prevent the electropolymerization of aniline in sulfuric acid solutions,

but that it can modify the physicochemical properties of the film (conductivity, morphology, and thickness), which could modulate the detection properties of polyaniline films [37].

Considering that the substrate is flexible, cross-section images of the PANI/H_2SO_4 sensors have been taken using SEM microscopy (Figure 2). The metallic stack formed by successive layers of Cu, Ni, and Au is clearly visible as well as the polyimide substrate. The thickness of the metallic stack can be estimated to approximately 20 µm from the image. The top and edges of this stack are coated by the polyaniline film, whose structure will be described below.

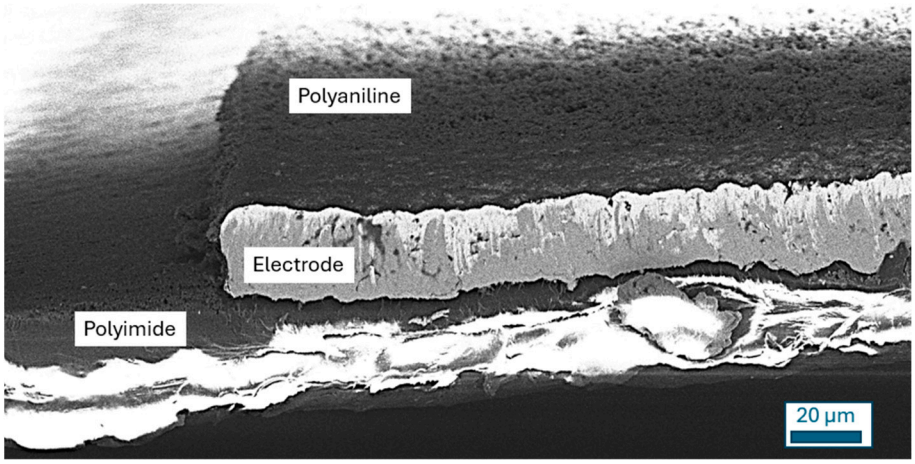

Figure 2. SEM cross-section image of a PANI/H_2SO_4 sensor.

The electrodes modified by polyaniline films were characterized in terms of thickness and morphology, as well as the uncoated gold electrodes. Thus, the thickness of 50 different gold electrodes was measured by mechanical profilometry. The obtained profiles showed a clear step between the substrate and the gold electrode (Figure 3a). The calculated average thickness, which is the sum of the thicknesses of the copper, nickel, and gold layers composing the electrode, was 20.52 µm (Table 1). The profiles obtained for the PANI/H_2SO_4 electrodes also showed a clear step (Figure 3b) and the average thickness of the whole system (gold electrode + PANI electrodeposited in H_2SO_4) calculated from 36 measurements was 21.12 µm, which corresponds to a polymer film of 0.60 µm. In the presence of surfactant and under the same operating conditions, the average thickness of polyaniline films was higher with an average value of 1.59 µm and 1.57 µm for the PANI/H_2SO_4 + CTAB and PANI/H_2SO_4 + Tritonx100 films, respectively. It is also noticeable that the standard deviation was the lowest for the PANI/H_2SO_4 films (Sd = 0.512) and the highest for the PANI/H_2SO_4 +CTAB films (Sd = 1.324).

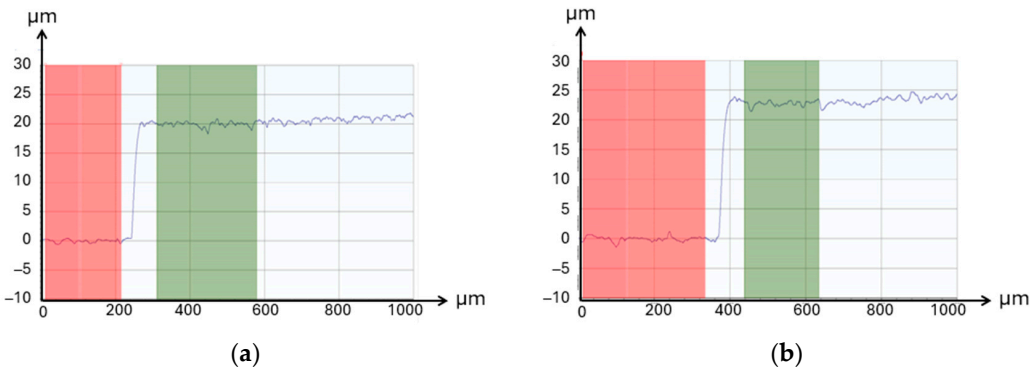

Figure 3. Step measurement of an uncoated electrode of the chip (**a**) and a PANI/H_2SO_4-modified electrode of the chip (**b**) obtained by stylus profilometry. Thicknesses were measured by subtracting the average height of the red zone (substrate) from the average height of the green zone (film).

Table 1. Thickness of the naked electrodes and of the different PANI-modified electrodes.

Samples	Average Thickness Value [1]	Standard Deviation
Naked electrodes	20.52 µm	0.477
PANI/H_2SO_4	21.12 µm	0.512
PANI/H_2SO_4 + CTAB	22.11 µm	1.324
PANI/H_2SO_4 + Tritonx100	22.09 µm	0.965

[1] Average value obtained from the measurements on 40 different sensors.

The topography of the different samples was then studied by SEM microscopy (Figure 4). The structure of the bare gold electrodes was fibrillary, compact, and dense enough to cover the entire surface of the electrodes (Figure 4a). The structure of PANI/H_2SO_4 films was also fibrillary and showed a high porosity, which is consistent with the structure generally observed for this polymer (Figure 4b). The structure of PANI/H_2SO_4 + CTAB films also exhibited a porosity, but lower, and was characterized by its great homogeneity (Figure 4c), whereas PANI/H_2SO_4 + Tritonx100 films showed a more inhomogeneous structure with some areas containing small nodules and other areas containing clusters of higher size, possibly because of the larger size of this surfactant (Figure 4d).

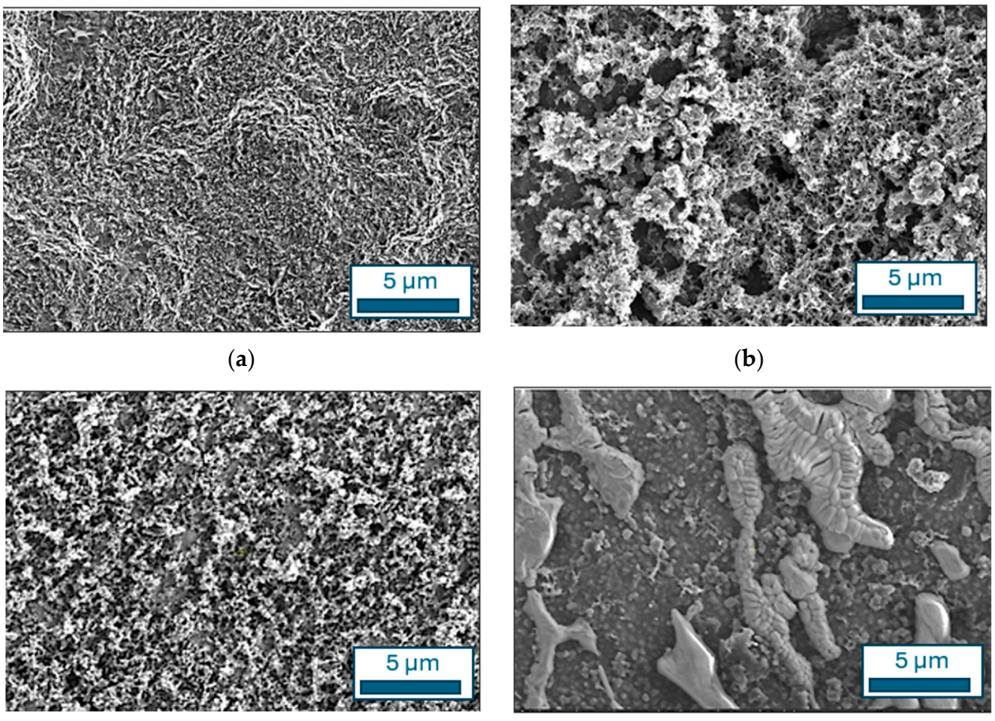

(**a**) (**b**) (**c**) (**d**)

Figure 4. SEM micrographs of an uncoated gold electrode (**a**), and of gold electrodes modified by a PANI/H_2SO_4 film (**b**), a PANI/H_2SO_4 + CTAB solution (**c**), or a PANI/H_2SO_4 + Tritonx100 solution (**d**).

3.2. Analytical Performance of the Potentiometric pH Sensors

3.2.1. Potentiometric Responses to pH Changes of Polyaniline-Based Sensors in Aqueous Solutions

For each sensor and for each pH value between 3 and 8, the evolution of the OCP as a function of time was measured for 60 s. Figure 5a gives the example of the OCP versus time curve for the PANI/H_2SO_4 sensor at pH 3. This curve shows that a duration of 60 s is sufficient to reach the equilibrium value of the OCP and that the measurements of the eight sensors are very similar, so the measurements are reproducible.

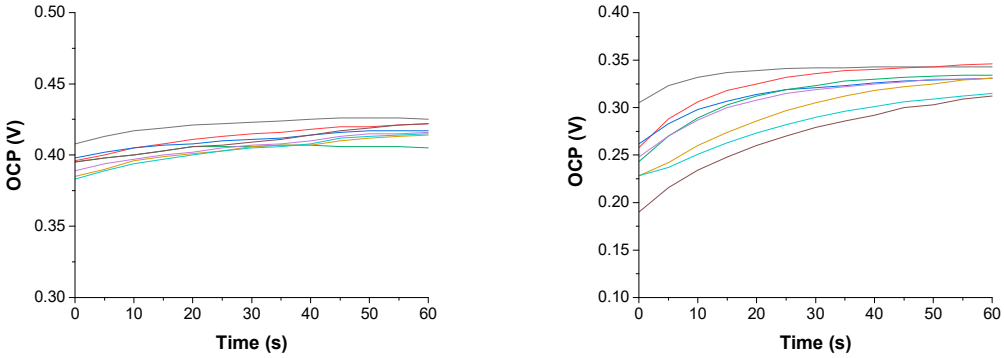

Figure 5. OCP versus time curves for PANI/H_2SO_4 sensor in the absence of hypochlorite ions at pH 3 (**a**) and OCP versus time curve for PANI/H_2SO_4 + Tritonx100 sensor in the presence of hypochlorite ions at pH 3 (**b**).

The responses to pH variations of eight PANI/H_2SO_4 sensors, deduced from the OCP versus time curves, are given in Figure 6a as well as the eight corresponding fitting lines. The fitting lines give access to the sensitivity of each sensor since the sensitivity of a pH sensor is defined as the slope of its calibrated line. Thus, it can be deduced from these OCP measurements that the sensitivity of the PANI-H_2SO_4 sensors varies from –70.5 mV per pH unit for the least sensitive sensor to –76.1 mV per pH unit for the most sensitive. The results also give an average sensitivity of –73.4 mV per pH unit with a standard deviation of 1.75 (Table 2). Therefore, these sensors can be considered very sensitive since their response is super-Nernstian (>59 mV per pH unit), and very reproducible since a low standard deviation is obtained. In addition, the sensing performance of the PANI-H_2SO_4 sensor appears excellent compared to the latest and most sensitive polyaniline sensors (Table 3). The addition of surfactant does not improve the potentiometric response of the sensors, since the average sensitivity obtained is 41.3 and 55.2 mV per pH unit for PANI films containing CTAB and Tritonx100, respectively (Figure 6b,c). Similarly, the reproducibility of the sensors is less good in the presence of surfactant since the standard deviation is 3.82 and 7.96 for PANI films containing CTAB and Tritonx100, respectively (Table 2). Figure 6d is obtained by averaging the potential measured by the eight electrodes for each pH and each sensor. The comparison of calibration curves shows unambiguously that PANI/H_2SO_4 sensors are the most sensitive to pH changes in the pH range from 3 to 8. The assumptions that may explain the highest sensitivity of PANI/H_2SO_4 sensors are: (i) a larger contact area of the film with hydrogen ions due to greater porosity of PANI/H_2SO_4 compared to the other films as can be deduced from the SEM images (Figure 4) and (ii) a number of amino sites allowing the detection of hydrogen ions lower in polyaniline films containing surfactants due to the place taken by surfactants in the film. The reversibility of the sensors was also evidenced through potential measurements and a difference of 15 mV or less has been measured according to the direction of measurement for the PANI/H_2SO_4 film, as well as the low drift of the measured potentials, since a low decrease of 14 mV was obtained after 8000 s for the PANI/H_2SO_4 film at pH 6.

Table 2. Equations of the calibrated curves of the pH sensors.

Samples	Without Hypochlorite	With Hypochlorite
PANI/H_2SO_4	OCP = 599.7–73.4 pH Sd = 1.75	OCP = 416.7–16.1 pH Sd = 12.93
PANI/H_2SO_4 + CTAB	OCP = 350.4–41.3 pH Sd = 3.82	OCP = 588.9–66.3 pH Sd = 4.10
PANI/H_2SO_4 + Tritonx100	OCP = 437.0–55.2 pH Sd = 7.96	OCP = 519.8–62.3 pH Sd = 1.52

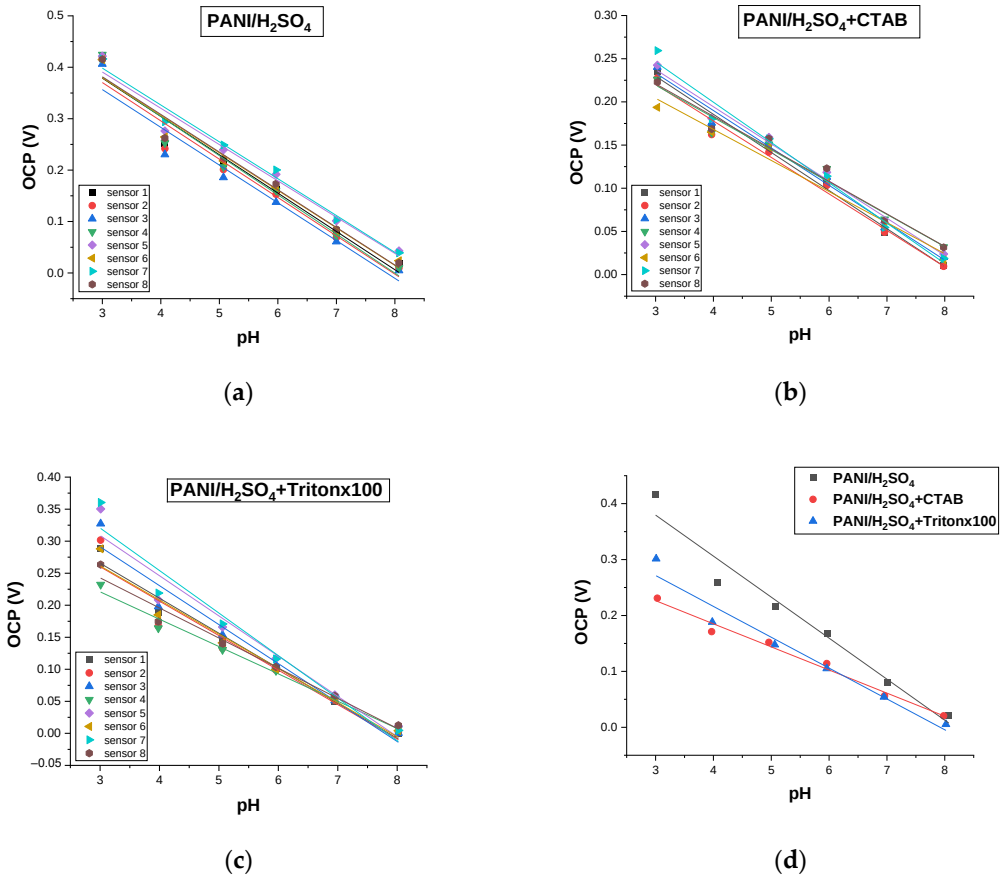

Figure 6. Potentiometric responses to pH changes of eight electrodes modified by PANI/H_2SO_4 (**a**), PANI/H_2SO_4 + CTAB (**b**), and PANI/H_2SO_4 + Tritonx1000 (**c**), as well as the average potentiometric responses to pH changes of the same electrodes (**d**).

Table 3. Comparison with other recent polyaniline-based pH sensors.

Sensing Material	Sensitivity mV/pH Unit	pH Range	Reference
PANI	62.3	2–8	[38]
PANI nanofibers	62.4	3–10	[35]
PANI + dodecyl benzene sulfonic acid	58.6	5.5–8.5	[36]
PANI + carbon	53.0	4–10	[39]
PANI + carbon nanofiber membrane	76.2	6.3–8.3	[40]
PANI nanopillars	60.3	2–12	[41]
PANI + HCl ink	69.1	4–10	[42]
PANI + phytic acid	69.3	4–9	[43]
PANI + MoS_2	70.4	4–8	[44]
PANI + TiO_2	66.1	2–12	[45]
PANI/H_2SO_4 + CTAB	41.3	3–8	This work
PANI/H_2SO_4 + Tritonx100	55.2	3–8	This work
PANI/H_2SO_4	73.4	3–8	This work

3.2.2. Potentiometric Responses to pH Changes of Polyaniline-Based Sensors in Oxidizing Solutions

Potentiometric responses to pH changes of sensors modified by the same polyaniline films as previously were then measured in the presence of hypochlorite. The presence of hypochlorite in the solution increases the Oxidation-Reduction Potential (ORP), which indicates the ability of the solution to be more oxidizing, meaning it has a greater tendency to accept electrons and undergo reduction reactions. Thus, in the pH range used for pH

tests, ORP ranged from 350 to 400 mV in the absence of hypochlorite ions in the solution, while it varied from 750 to 1100 mV in the presence of hypochlorite ions. Hypochlorite ions can interfere with the measurement of pH in aqueous solutions, since they can react with water to form hypochlorous acid and hydroxide ions (1). So, the presence of hypochlorite ions induces an increase of the concentration of hydroxide ions in the solution, which in turn affects the measured pH, leading to a pH value different from that which would be expected solely based on the concentration of the original acid or base present in the solution.

$$ClO^- + H_2O \rightleftharpoons HOCl + OH^- \quad (1)$$

Moreover, the presence of hypochlorite ions can cause an oxidation of the polyaniline electrodeposited on the sensors, and therefore, affect the potential measurements as a function of the pH.

The consequences of the addition of hypochlorite ions in the analyte solution is the increase of the time required to reach the equilibrium value of the potential as can be seen on the curves giving the evolution of the OCP versus the time for eight PANI/H_2SO_4 + Tritonx100 sensors (Figure 5b) as well as a decrease of the reversibility of the pH sensors.

Figure 7a,b also indicate clearly that the potentiometric responses to pH changes of the eight PANI/H_2SO_4 sensors is strongly affected by the presence of hypochlorite ions in the solutions. It can even be considered that these films no longer play their role of sensors because of the interference generated by hypochlorite ions via the phenomena previously described. PANI/H_2SO_4 + CTAB sensors are also affected by the presence of hypochlorite ions but in a much less marked way (Figure 7c,d). Their sensitivity to pH changes is high but the response is not linear over the entire pH range and reproducibility is not completely satisfactory as evidenced by the high standard deviation (Sd = 4.10, Table 2). On the contrary, the PANI/H_2SO_4 + Tritonx100 sensors maintain a sensor behavior even in the presence of hypochlorite. Their response remains perfectly linear (Figure 7e,f), their sensitivity is high (62.3 mV per pH unit), and the reproducibility of the response is very satisfactory (Sd = 1.52). Thus, while the PANI/H_2SO_4 sensors were the most efficient in aqueous solution, it appears that the PANI/H_2SO_4 + Tritonx100 sensors are by far the most efficient in oxidizing solution. A possible explanation for the deterioration of the response of some sensors could be the corrosion of polyaniline films in an oxidizing medium. Since the films of PANI/H_2SO_4 + CTAB and even more the films of PANI/H_2SO_4 are more porous than the PANI/H_2SO_4 + Tritonx100 films (Figure 4), it may be assumed that the hypochlorite ions could penetrate the pores of the films of PANI/H_2SO_4 + CTAB and PANI/H_2SO_4 and causes corrosion of Cu/Ni/Au stacks or PANI films. However, the photographs of PANI/H_2SO_4 and PANI/H_2SO_4 + CTAB sensors that were carried out at the end of a series of tests in solutions containing hypochlorite ions did not reveal any marked deterioration, only small traces of corrosion, especially on the edges of the electrodes (Figure 8a,b). It is also possible that hypochlorite ions penetrate the pores of the films of PANI/H_2SO_4, leading to a decrease of the specific surface area capable of detecting hydrogen ions. On the contrary, the addition of a surfactant reduces the penetration of hypochlorite ions, since the structure of the PANI/H_2SO_4 + CTAB film is less porous than the one of the PANI/H_2SO_4 film, while the structure of the PANI/H_2SO_4 + Tritonx100 film is not porous at all and prevents the penetration of hypochlorite ions into the pores and allows the obtention of the best pH sensing properties. However, if pH sensors based on PANI/H_2SO_4 + Tritonx100 are sensitive and reproducible in the presence of hypochlorite ions, exposure to such an oxidizing medium reduces their reactivity, resulting in lower stability over time and difficulty to maintaining their response at the same level of sensitivity after multiple uses. Therefore, it is better to consider using them as single-use pH sensors, which is made possible by the fact that we use an inexpensive manufacturing process.

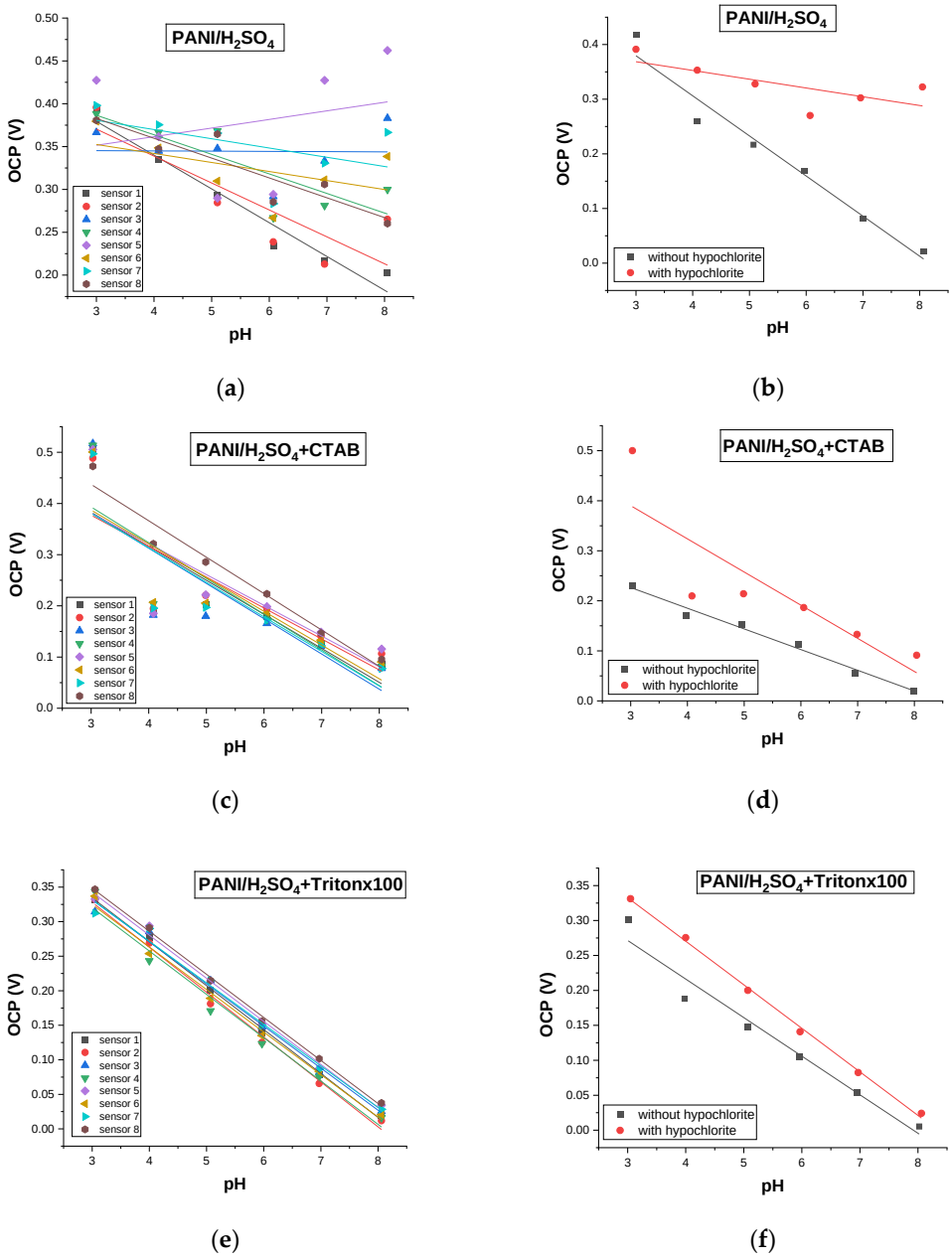

Figure 7. Potentiometric responses to pH changes in the presence of hypochlorite ions of eight electrodes modified by PANI/H_2SO_4 (**a**), PANI/H_2SO_4 + CTAB (**c**), and PANI/H_2SO_4 + Tritonx1000 (**e**), as well as the average potentiometric responses to pH changes of the same electrodes (**b**,**d**,**f**).

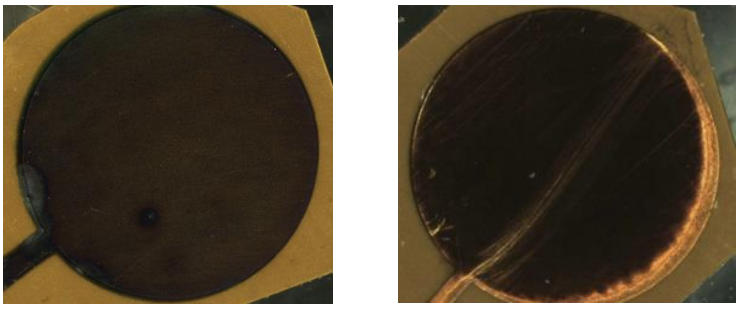

(**a**) (**b**)

Figure 8. Photographs of PANI/H_2SO_4 (**a**) and PANI/H_2SO_4 + CTAB (**b**) sensors at the end of a series of tests in solutions containing hypochlorites.

4. Conclusions

In this work, flexible polyaniline-based sensors were prepared for potentiometric pH measurements in aqueous and oxidizing solutions. Flexible polyimide-copper-nickel-gold electrodes were manufactured and employed as substrates for the electrodeposition of polyaniline. The resulting sensors were tested as pH sensors by measuring the OCP value over a wide range of pH going from 3 to 8. The PANI/H_2SO_4 sensors showed good reproducibility (Sd = 1.75) and high super-Nernstian sensitivity (73.4 mV per unit pH) in aqueous solutions, but they exhibited poorly reproducible and nonlinear potentiometric responses to pH changes in aqueous solutions containing hypochlorite ions, maybe because of the insertion of the hypochlorite anions into the numerous pores of the polyaniline film. To solve this problem, other electrolyte compositions, including CTAB or Tritonx100, have been used to electrodeposit polyaniline films with less porous morphologies, and thus, they are potentially less susceptible to trapping hypochlorite ions that may disturb pH detection by acting as interferents of hydrogen ions or as oxidizing agent of polyaniline films. This strategy has been successful, since the potentiometric responses of PANI/H_2SO_4 + Tritonx100 sensors were highly sensitive (62.3 mV per unit pH) and reproducible (standard deviation of 1.52) over the pH range going from pH 3 to 8. This study, therefore, shows that it is possible to manufacture sensitive flexible pH sensors using conductive polymers as active layers. However, it is sometimes necessary to optimize the composition of the electrolyte according to the medium, oxidizing or not, in which the measurements are made in order to electrodeposit a polymer film with optimal detection properties.

Author Contributions: Conceptualization, C.R. and S.V.; methodology, L.B. and C.R.; investigation, L.B., C.M. and S.L.; writing—original draft preparation, B.L.; writing—review and editing, B.L. and C.R.; supervision, C.R.; project administration, S.V. and B.L. All authors have read and agreed to the published version of the manuscript.

Funding: This research received no external funding.

Institutional Review Board Statement: Not applicable.

Informed Consent Statement: Not applicable.

Data Availability Statement: All created data are included in the manuscript.

Acknowledgments: This work was supported by the instruments and staff of the UTINAM Chemistry technical Platform (PCU). This work was also partly supported by the French RENATECH network and its FEMTO-ST technological facility.

Conflicts of Interest: Author Liam Bignall, Catheline Ramsamy and Simon Vassal were employed by the company Linxens Holding. The remaining authors declare that the research was conducted in the absence of any commercial or financial relationships that could be construed as a potential conflict of interest.

References

1. Sorensen, S.P.L. Enzymstudien. II, Über die Messung und die Bedeutung der Wasserstoffionenkonzentration bei enzymatischen Prozessen. *Biochem. Z.* **1909**, *21*, 131–304.
2. Hückel, E.; Debye, P. The theory of electrolytes: I. lowering of freezing point and related phenomena. *Phys. Z.* **1923**, *24*, 185–206.
3. Marczewska, B.; Marczewski, K. First Glass Electrode and its Creators F. Haber and Z. Klemensiewicz—On 100th Anniversary. *Z. Phys. Chem.* **2010**, *224*, 795–799. [CrossRef]
4. Thackray, A.; Myers, M., Jr. *Arnold O. Beckman: One Hundred Years of Excellence*; Chemical Heritage Foundation: Philadelphia, PA, USA, 2000; 397p.
5. Chesler, M. Regulation and modulation of pH in the brain. *Phys. Rev.* **2003**, *83*, 1183–1221. [CrossRef] [PubMed]
6. Li, Z.; Sun, C.; Lou, L.; Li, Z. Endogenous microenvironmental engineering through targeted alteration of salt bridge network can effectively regulate enzymatic pH adaptation. *Chem. Eng. J.* **2022**, *442*, 136215. [CrossRef]
7. Li, K.T.; Liu, D.H.; Chu, J.; Wang, Y.H.; Zhuang, Y.P.; Zhang, S.L. An effective and simplified pH-stat control strategy for the industrial fermentation of vitamin B 12 by Pseudomonas denitrificans. *Bioproc. Biosyst. Eng.* **2008**, *31*, 605–610. [CrossRef] [PubMed]
8. Antonacci, A.; Arduini, F.; Moscone, D.; Palleschi, G.; Scognamiglio, V. Commercially available (bio) sensors in the agrifood sector. *Compr. Anal. Chem.* **2016**, *74*, 315–340. [CrossRef]

9. Penn, C.J.; Camberato, J.J. A critical review on soil chemical processes that control how soil pH affects phosphorus availability to plants. *Agriculture* **2019**, *9*, 120. [CrossRef]
10. Husson, O. Redox potential (Eh) and pH as drivers of soil/plant/microorganism systems: A transdisciplinary overview pointing to integrative opportunities for agronomy. *Plant Soil* **2013**, *362*, 389–417. [CrossRef]
11. Saalidong, B.M.; Aram, S.A.; Otu, S.; Lartey, P.O. Examining the dynamics of the relationship between water pH and other water quality parameters in ground and surface water systems. *PLoS ONE* **2022**, *17*, e0262117. [CrossRef]
12. Swain, S.; Sawant, P.B.; Chadha, N.K.; Chhandaprajnadarsini, E.M.; Katare, M.B. Significance of water pH and hardness on fish biological processes: A review. *Int. J. Chem. Stud.* **2020**, *8*, 330–337. [CrossRef]
13. Wencel, D.; Abel, T.; McDonagh, C. Optical chemical pH sensors. *Anal. Chem.* **2014**, *86*, 15–29. [CrossRef]
14. Steinegger, A.; Wolfbeis, O.S.; Borisov, S.M. Optical sensing and imaging of pH values: Spectroscopies, materials, and applications. *Chem. Rev.* **2020**, *120*, 12357–12489. [CrossRef]
15. Kneipp, J.; Kneipp, H.; Wittig, B.; Kneipp, K. Novel optical nanosensors for probing and imaging live cells. *Nanomedicine* **2010**, *6*, 214–226. [CrossRef]
16. Sinha, S.; Pal, T. A comprehensive review of FET-based pH sensors: Materials, fabrication technologies, and modeling. *Electrochem. Sci. Adv.* **2022**, *2*, e2100147. [CrossRef]
17. Shojaei Baghini, M.; Vilouras, A.; Douthwaite, M.; Georgiou, P.; Dahiya, R. Ultra-thin ISFET-based sensing systems. *Electrochem. Sci. Adv.* **2022**, *2*, e2100202. [CrossRef]
18. Sahu, N.; Bhardwaj, R.; Shah, H.; Mukhiya, R.; Sharma, R.; Sinha, S. Towards development of an ISFET-based smart pH sensor: Enabling machine learning for drift compensation in IoT applications. *IEEE Sens. J.* **2021**, *21*, 19013–19024. [CrossRef]
19. Mello, H.J.N.P.D.; Mulato, M. Influence of galvanostatic electrodeposition parameters on the structure-property relationships of polyaniline thin films and their use as potentiometric and optical pH sensors. *Thin Solid Films* **2018**, *656*, 14–21. [CrossRef]
20. Fraga, V.M.; Lovi, I.T.; Abegao, L.M.; Mello, H.J. Understanding the Effect of Deposition Technique on the Structure–Property Relationship of Polyaniline Thin Films Applied in Potentiometric pH Sensor. *Polymers* **2023**, *15*, 3450. [CrossRef]
21. Zuaznabar-Gardona, J.C.; Fragoso, A. A wide-range solid state potentiometric pH sensor based on poly-dopamine coated carbon nano-onion electrodes. *Sens. Actuators B* **2018**, *273*, 664–671. [CrossRef]
22. Taouil, A.E.; Lallemand, F.; Melot, J.M.; Husson, J.; Hihn, J.Y.; Lakard, B. Effects of polypyrrole modified electrode functionalization on potentiometric pH responses. *Synth. Met.* **2010**, *160*, 1073–1080. [CrossRef]
23. Wang, Y.; Liu, A.; Han, Y.; Li, T. Sensors based on conductive polymers and their composites: A review. *Polym. Int.* **2020**, *69*, 7–17. [CrossRef]
24. Manjakkal, L.; Dervin, S.; Dahiya, R. Flexible potentiometric pH sensors for wearable systems. *RSC Adv.* **2020**, *10*, 8594–8617. [CrossRef]
25. Alam, A.U.; Qin, Y.; Nambiar, S.; Yeow, J.T.; Howlader, M.M.; Hu, N.X.; Deen, M.J. Polymers and organic materials-based pH sensors for healthcare applications. *Progr. Mater. Sci.* **2018**, *96*, 174–216. [CrossRef]
26. Liu, L.; Zhang, X. A focused review on the flexible wearable sensors for sports: From kinematics to physiologies. *Micromachines* **2022**, *13*, 1356. [CrossRef]
27. Sun, W.; Guo, Z.; Yang, Z.; Wu, Y.; Lan, W.; Liao, Y.; Wu, X.; Liu, Y. A review of recent advances in vital signals monitoring of sports and health via flexible wearable sensors. *Sensors* **2022**, *22*, 7784. [CrossRef]
28. Chen, S.; Qi, J.; Fan, S.; Qiao, Z.; Yeo, J.C.; Lim, C.T. Flexible wearable sensors for cardiovascular health monitoring. *Adv. Healthc. Mater.* **2021**, *10*, 2100116. [CrossRef]
29. Cheng, M.; Zhu, G.; Zhang, F.; Tang, W.L.; Jianping, S.; Yang, J.Q.; Zhu, L.Y. A review of flexible force sensors for human health monitoring. *J. Adv. Res.* **2020**, *26*, 53–68. [CrossRef]
30. Goswami, P.; Gupta, G. Recent progress of flexible NO_2 and NH_3 gas sensors based on transition metal dichalcogenides for room temperature sensing. *Mater. Today Chem.* **2022**, *23*, 100726. [CrossRef]
31. Bag, A.; Lee, N.E. Recent advancements in development of wearable gas sensors. *Adv. Mater. Technol.* **2021**, *6*, 2000883. [CrossRef]
32. Ouyang, J. Application of intrinsically conducting polymers in flexible electronics. *SmartMat* **2021**, *2*, 263–285. [CrossRef]
33. Pavel, I.A.; Lakard, S.; Lakard, B. Flexible sensors based on conductive polymers. *Chemosensors* **2022**, *10*, 97. [CrossRef]
34. Lin, J.C.; Liatsis, P.; Alexandridis, P. Flexible and stretchable electrically conductive polymer materials for physical sensing applications. *Polym. Rev.* **2023**, *63*, 67–126. [CrossRef]
35. Park, H.J.; Yoon, J.H.; Lee, K.G.; Choi, B.G. Potentiometric performance of flexible pH sensor based on polyaniline nanofiber arrays. *Nano Converg.* **2019**, *6*, 9. [CrossRef]
36. Li, Y.; Mao, Y.; Xiao, C.; Xu, X.; Li, X. Flexible pH sensor based on a conductive PANI membrane for pH monitoring. *RSC Adv.* **2020**, *10*, 21–28. [CrossRef]
37. Kayishaer, A.; Magnenet, C.; Pavel, I.A.; Halima, H.B.; Moutarlier, V.; Lakard, B.; Redon, N.; Duc, C.; Lakard, S. Influence of surfactant on conductivity, capacitance and doping of electrodeposited polyaniline films. *Front. Mater.* **2024**, *11*, 1358534. [CrossRef]
38. Mazzara, F.; Patella, B.; D'Agostino, C.; Bruno, M.G.; Carbone, S.; Lopresti, F.; Aiello; Torino, C.; Vilasi, A.; O'Riordan, A.; et al. PANI-based wearable electrochemical sensor for pH sweat monitoring. *Chemosensors* **2021**, *9*, 169. [CrossRef]

39. Rahimi, R.; Ochoa, M.; Tamayol, A.; Khalili, S.; Khademhosseini, A.; Ziaie, B. Highly stretchable potentiometric pH sensor fabricated via laser carbonization and machining of Carbon−Polyaniline composite. *ACS Appl. Mater. Interfaces* **2017**, *9*, 9015–9023. [CrossRef]
40. Lu, H.; Lei, T.; Zhang, L.; Chen, S.; Chen, R.; Li, X.; Wang, Y.; Zhu, J.; Chen, M.; Zhang, K.; et al. Flexible polyaniline@ carbon nanofiber membrane pH electrode for health care. *Microchem. J.* **2024**, *200*, 110436. [CrossRef]
41. Yoon, J.H.; Hong, S.B.; Yun, S.O.; Lee, S.J.; Lee, T.J.; Lee, K.G.; Choi, B.G. High Performance Flexible pH Sensor Based on Polyaniline Nanopillar Array Electrode. *J. Colloid Interface Sci.* **2017**, *490*, 53–58. [CrossRef]
42. Bilbao, E.; Kapadia, S.; Riechert, V.; Amalvy, J.; Molinari, F.N.; Escobar, M.M.; Baumann, R.R.; Monsalve, L.N. Functional aqueous-based polyaniline inkjet inks for fully printed high-performance pH-sensitive electrodes. *Sens. Actuators B* **2021**, *346*, 130558. [CrossRef]
43. Madeira, G.D.M.; Dias Mello, H.J.; Faleiros, M.C.; Mulato, M. Model improvement for super-Nernstian pH sensors: The effect of surface hydration. *J. Mater. Sci.* **2021**, *56*, 2738–2747. [CrossRef]
44. Choudhury, S.; Deepak, D.; Bhattacharya, G.; McLaughlign, J.; Roy, S.S. MoS_2-Polyaniline Based Flexible Electrochemical Biosensor: Toward pH Monitoring in Human Sweat. *Macromol. Mat. Eng.* **2023**, *308*, 2300007. [CrossRef]
45. Kamarozaman, N.S.; Zainal, N.; Rosli, A.B.; Zulkefle, M.A.; Nik Him, N.R.; Abdullah, W.F.H.; Herman, S.H.; Zulkifli, Z. Highly sensitive and selective sol-gel spin-coated composite TiO_2–PANI thin films for EGFET-pH sensor. *Gels* **2022**, *8*, 690. [CrossRef]